BEFIB2012 – Fibre reinforced concrete
Joaquim Barros et al. (Eds)
 UM, Guimarães, 2012

ASSESSMENT OF FIBRE ORIENTATION AND DISTRIBUTION IN STEEL FIBRE REINFORCED SELF-COMPACTING CONCRETE PANELS

A. Abrishambaf[*1], J.A.O. Barros[*2], V.M.C.F. Cunha[†] and F.N.M. Cunha[₸]

[*] ISISE, Dep. Civil Eng., School Eng., University of Minho
Campus de Azurém 4800-058 Guimarães, Portugal
e-mail: [1]amin.abrishambaf@yahoo.com, [2]barros@civil.uminho.pt, web page: www.isise.net

[†] ISISE, Dep. Eng., Faculty of Sciences and Tech., University of Trás-os-Montes e Alto Douro
Quinta de Prados, 5001-801, Vila Real, Portugal
e-mail: vcunha@utad.pt, web page: www.isise.net

[₸] ISISE, CiviTest Company, Pesquisa de Novos Materiais para a Engenharia Civil
Rua Joaquim de Sá Leonardo, Pavilhão 3 – Antas, 4760-042 Vila Nova de Famalicao, Portugal
e-mail: fredericocunha@civitest.com, web page: www.civitest.pt

Keywords: Steel fibres, Fibre orientation, Fibre dispersion, Splitting (indirect) tensile test, Self-compacting concrete.

Summary: *The benefits of adding fibres to concrete lie, mostly, in improving the post-cracking behaviour, since its ability to transfer stresses across cracked sections is substantially increased. The post-cracking strength is dependent not only on the fibre geometry, mechanical performance and fibre/matrix interface properties, but also on the fibre orientation and distribution. Previous works have shown that in self-compacting concrete matrices, there is a preferential fibre alignment according to the concrete's flow in the fresh state. Having in mind that fibres are more efficient if they are oriented according the principal tensile stresses, a preferential fibre alignment on a certain direction could either enhance or diminish the material and the structural performance of this composite. In this paper, it is investigated the influence of the fibre orientation and distribution on the post-cracking behaviour of the steel fibre reinforced self-compacting concrete (SFRSCC). To perform this evaluation, SFRSCC panels were casted from their centre point. Two self-compacting mixtures were prepared using the same base mix proportions. For each SFRSCC panel cylindrical specimens were extracted and the post-cracking behaviour was assessed from a crack width controlled splitting tensile test.*

1 INTRODUCTION

Steel fibre reinforced self-compacting concrete (SFRSCC) is a material that can flow under its own weight and fill formwork without the need for any type of internal or external vibration. This kind of concrete mix can mitigate two current concrete weaknesses: low workability in fibre reinforced concretes and reduced cracking resistance in plain concrete. The enhanced properties of SFRSCC enable to step up both the constructive process and the material mechanical properties. By the utilization of SFRSCC, bleeding and segregation, which may exist due to improper vibration and may reduce the fibre/matrix bond strength, can be avoided [1].

The addition of fibres to a cementicious matrix may contribute to improve the energy absorption and ductility, load transfer capacity, residual load bearing capacity, durability, fire and impact resistance, e.g. [2-4]. The post-cracking strength is dependent not only on the fibre properties (their tensile and bond strength, stiffness and geometry), but also on their orientation and distribution within the concrete bulk. The number of effective fibres at the fracture surface influences mostly the tensile residual stress in the post-cracking phase. Moreover, the scatter commonly observed on the residual

strength of fibre reinforced composites can be ascribed to the random nature of the fibre dispersion, in particular, to the variation of the fibre density and orientation at the crack surface [4-6].

As previously stated, the contribution of fibres to bridge stresses across a crack depends not only on the uniformity of the fibre dispersion, but also on their orientation. Several researchers have observed that fibre orientation and dispersion are a consequence of a multiplicity of factors, namely fresh-state properties, casting conditions into the formwork, flowability characteristics, vibration and wall-effect introduced by the formwork [7,8]. Among these factors, the most important ones for SFRSCC are the wall effects introduced by the formwork, the fresh state properties (flowability) of self-compacting concrete, SCC, and casting process [7-9]. Previous works have shown that in self-compacting concretes there is a preferential fibre alignment according the concrete's flow in the fresh state [3,4,8]. Thus, in order to potentiate the high flowability of SCC, it would be desirable that the concrete flow direction and, therefore, the alignment of fibres should be as close as possible to the directions of the principal tensile stresses, in order to increase the number of effective fibres to face up these stresses when cracks are forming.

In this paper, it is investigated the influence on the SFRSCC post-cracking behaviour of the concrete meso-structural characteristics, particularly the type, orientation and distribution of fibres. To perform this evaluation, two SFRSCC panels were casted using the same base mix proportions. Core specimens were extracted at distinct distances from the casting point, and they were submitted to indirect tensile tests for the evaluation of the influence of fibre density and orientation on the stress-crack width relationship of this composite.

2 ASSESSMENT OF THE STRESS-CRACK WIDTH RELATIONSHIP BY INDIRECT TENSILE TESTS

The splitting tensile test, also known as Brazilian or indirect tensile test is a widely standard test used to determine the tensile strength of concrete. This test method is mentioned in several international concrete standards such as: ASTM C-496, ISO 4108-1980 and BS 1981: Part 117. In this test, a compressive load is applied along two diametrically opposite line loads of a cylindrical or prismatic specimen. The compressive load induces a linear tensile stress state perpendicular to the loading plane at the central part of the specimen [10]. After reaching the tensile strength in this zone, the micro-cracks coalescence, the crack starts to grow towards the loading strips.

To prevent crushing at the points of loading, two bearing strips may be used in order to distribute the applied load. In the case of a material with linear-elastic behaviour, due to the geometry of the specimen a theoretical uniform tensile stress along the plane of loading is installed that leads to the rupture of the specimen in two halves [11]. However, since fibre reinforced concrete is a pseudo-ductile material, and in this composite residual strength does not depend only on fibre content and type of the fibres but also on the distribution and orientation of fibres, therefore stress distribution along the centre of the specimen will not be uniform.

In the case of applying load directly on the specimen, the maximum tensile strength exists in the centre of the specimen and can be calculated by:

$$\sigma = \sigma_{sp} = \frac{2F}{\pi DL} \tag{1}$$

where F is the maximum applied line load, D is the diameter of the specimen (150 mm) and L is the length of the net area in the notched plane (about 50 mm).

2.1 Production and properties of steel fibre reinforced self-compacting concrete

Two SFRSCC panels were prepared from the same base mixture. The mix constituent materials are Portland cement CEM 42.5 R, water, superplasticizer Sika® 3005, limestone filler, crushed granite aggregate, fine and coarse sand, and steel fibres. The mix proportions are shown in Table 1. The SCC1 batch incorporates 35 mm long and 0.53 mm diameter with aspect ratio of 65 hooked-end steel

fibres, while in SCC2 batch are used approximately similar fibres with 33 mm length, 0.55 mm diameter and aspect ratio of 60. Both fibres have a tensile strength around 1100 MPa, and a content of 60 kg/m^3 of fibres was used in both batches.

Table 1: Mix proportions of steel fibre reinforced self-compacting concrete per m^3

Mixture	Cement [kg]	Water [kg]	W/C [–]	SP [kg]	Filler [kg]	Fine sand [kg]	Coarse sand [kg]	Coarse aggregate [kg]	Fibre [kg]
SCC1	412	124	0.30	7.83	353	179	655	588	60
SCC2	413	140	0.34	7.83	353	237	710	590	60

To have a SFRSCC with properties as closest as possible to those that can be found in a real structural application, the SFRSCC was made in industrial conditions. After the mixing procedure, the SFRSCC was introduced into a mixing-truck, and transported to the location of the slab moulds. The self-compacting requisites of the material were evaluated before casting the SFRSCC panels. The inverted Abrams cone slump test was performed according to EFNARC recommendations [12]. Slump values of 62 and 67 cm were achieved for SCC1 and SCC2 respectively. In SCC1 some segregation was observed, whereas for SCC2 the desired homogeneity and aggregate dispersion was achieved.

Each slab was casted from its centre point and measured 1600 × 1000 mm^2 in plan with a 60 mm thickness. The fresh concrete was unloaded directly from the mixing-truck by an U-shape channel and poured to the centre of the mould from the height of 600 mm. In the case of the SCC1 batch, due to the segregation problems, the material could not fill the mould properly. Therefore, after casting, some more concrete was added to the slab corners in order to properly fill the mould. After 24 hours, specimens were removed from the moulds, covered with wet sacks for one week and kept in a controlled temperature air room. In addition, for each batch, mechanical properties in compression and flexure were determined using 150 mm diameter cylinder and 150×150×600 mm beams after 28 days of moist curing (Table 2). To determine the effects of dispersion and orientation of fibres on the stress-crack opening relationship, σ-w, from indirect tensile test, 23 cylindrical specimens with a diameter of 150 mm were cored from each slab, according to the scheme shown in Figure 1. In this plan, the arrangement of the cores is based on the supposed concrete flow direction. Notches with distinct orientations (θ) 0° and 90° (the notched plane is parallel and ort hogonal to the direction of flow, respectively) were made on the lateral surfaces of each core (see Figure 1), in order to evaluate the influence of the crack plane orientation on the σ-w relationship. For instance θ of D1 and D6 specimens is 90° and 0°, respectively. The width and depth of the notches were 5 mm. Since panels were casted from the centre point (point O in Figure 1), by assuming this point as origin, due to the symmetry in the panels, each core was notched in the opposite direction of its symmetry pair in order to assess the effects of fibre orientation on the tensile behaviour of the material.

Table 2: Mechanical properties in compression and flexure tests (numbers in parentheses represent coefficient of variation)

	Properties in compression		Residual strength parameters in flexural test			
Mixture	f_C' [MPa]	E [GPa]	f_{R1} [MPa]	f_{R2} [MPa]	f_{R3} [MPa]	f_{R4} [MPa]
SCC1	69.25 (3.95%)	35.45 (5.78%)	9.00	4.45	2.60	1.77
SCC2	47.77 (7.45%)	34.15 (0.21%)	9.15	11.34	9.08	7.54

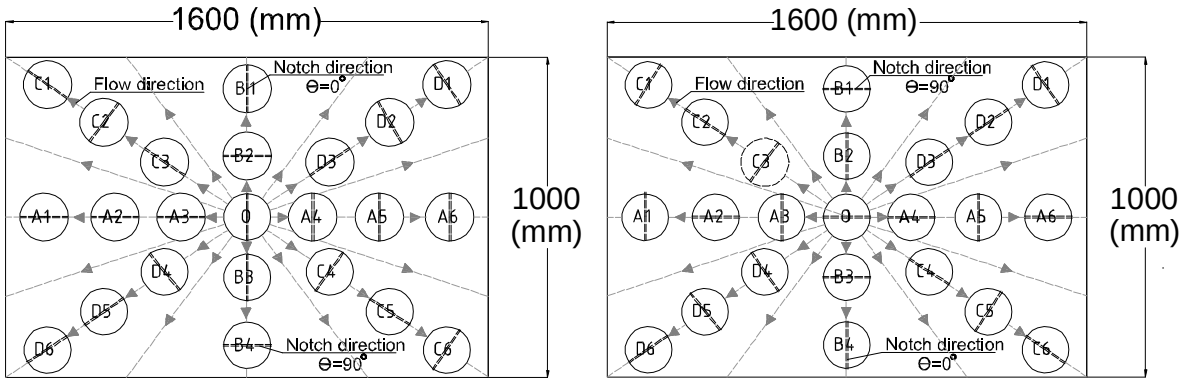

(a) (b)

Figure 1: Core extracting plan: (a) for SCC1 and (b) for SCC2 (pale dash lines with arrows represent concrete flow direction)

2.2 Test setup

The SFRSCC stress-crack opening relationship was assessed by splitting tests based on ASTM C496 standard [13]. The tests were carried out in displacement-control on an universal testing rig with a bearing capacity of 150 kN. The tests were performed in a relatively low displacement rate of 0.001 mm/sec. An external displacement transducer positioned on the actuator that measured the vertical deformation of the specimen was used to control the test. The applied load and crack-opening tip displacement were recorded on a data acquisition system.

Each drilled core is positioned between two supports and a compressive line load is applied along the thickness of the specimen until failure occurs. This applied load induces tensile stresses in the major part of the notched plane, and also a relatively high compressive stresses in the area around the supports. The test setup is depicted in Figure 2.

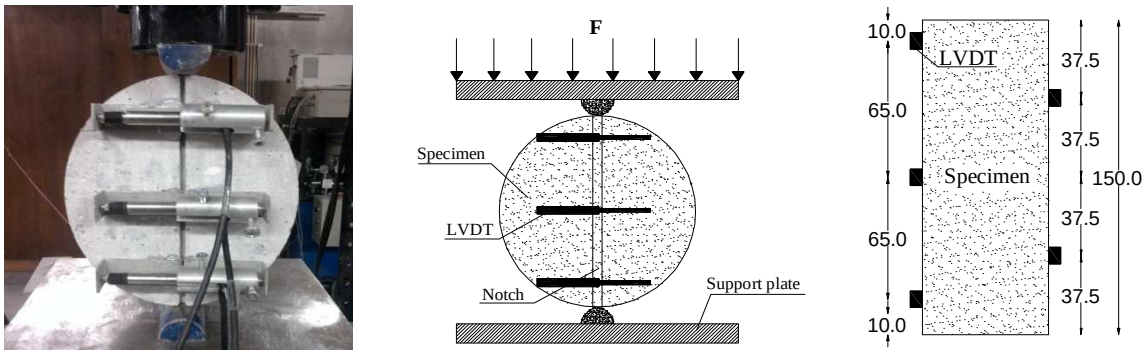

(a) (b) (c)

Figure 2: Geometry of the specimen and setup of the indirect tensile test (dimensions are in mm): (a) General view, (b) Specimen front view (top of the panel) and (c) Specimen lateral view

Five displacement transducers (LVDTs) were positioned on specimens to record crack opening along the specimen's height. To assess if unsymmetric crack oppening occurs, due to fibre segregation during the casting procedure, two LVDTs were located at the specimen's bottom surface, while the others were fixed on the top surface of the core.

2.3 Result and discussion

Figures 3 and 4 depict the nominal stress – crack opening mouth displacement relationship, σ – w, both envelope and average curves, for specimens extracted from distinct locations of the panel prototypes (Figure 1). The crack opening mouth displacement (w) was obtained by averaging the crack opening width recorded in the 5 LVDTs applied in each specimen. The nominal stress is calculated from Equation 1. Due to the segregation problems and therefore, non-homogeneity distribution of the aggregates and fibres in the batch SCC1, specimens A1, A6, B3, C4, C6, D1 and D6 failed in the crack initiation step during the test. Most of these specimens are located near the corner of the panel at the maximum distance from the casting point (centre of the slab).

For both tested series, the σ - w response is almost linear up to the stress at crack initiation. Up to this stress level, the displacements recorded by the LVDTs represent the deformability of the SFRSCC volume in the notched zone (between the supports of the LVDTs). Therefore, the deformability during this first phase would have been removed from the σ - w response, but due to its negligible value this was not done. After crack initiation, the σ - w response is nonlinear up to peak load. Once the peak load is attained, the load smoothly decreases (softening behaviour) up to a minimum post-peak stress. The decrease in the residual stresses is more noticeable in the case of SCC1, since this mixture has shown higher compressive strength. In this case, due to a higher bond strength between matrix and fibre interface, more fibres ruptured, while in the SCC2 due to the lower stiffness of the matrix, they did not fracture so often as in the SCC1 series, and the fibres could be fully pulled-out. With a less significant point of view, in SCC2 fibres with lower aspect ratio (smaller length and larger diameter) were used, which favored the non-occurrence of fiber rupture. Consequently, for the SCC2 series, the residual stresses increased due to the full mobilization of the hooked-end, in particular for the series with the notch parallel to the concrete flow direction ($\theta = 0^{\circ}$).

The average tensile strength obtained from the maximum load during splitting tests is 3.96 MPa and 3.40 MPa, respectively, for the SCC1 and SCC2, see Table 3. However, for both series, the scatter observed in the tensile strength was high, particularly in the specimens with the notch perpendicular to the flow direction ($\theta = 90^{\circ}$) for the SCC2 series, and ranged from 1.46 to 3.90 MPa.

Table 3: Tensile strength obtained from the splitting tests (MPa) (numbers in parentheses represent coefficient of variation)

Batch	$\theta = 0^{\circ}$	$\theta = 90^{\circ}$	Average
SCC 1	4.23 (29.68 %)	3.69 (14.96 %)	3.96
SCC 2	4.39 (28.11 %)	2.42 (47.40 %)	3.40

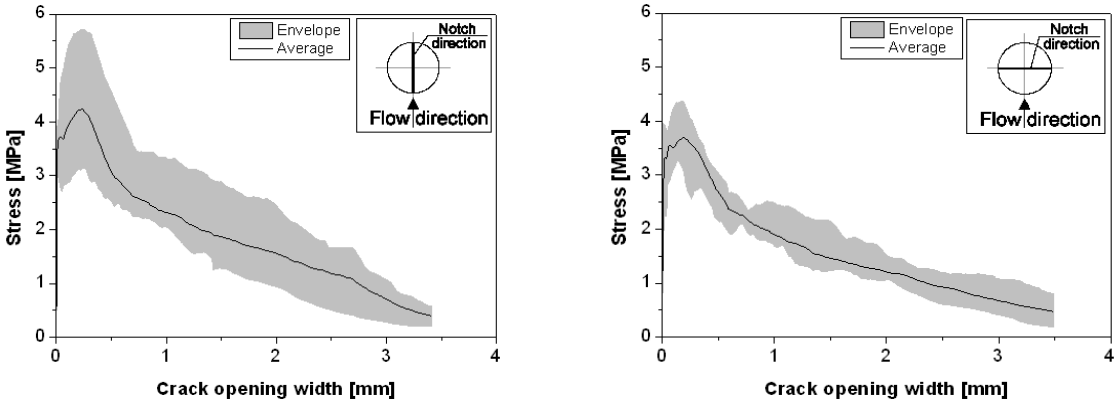

Figure 3: Nominal tensile stress – crack opening width relationship for SCC1: (a) $\theta = 0^{\circ}$ and (b) $\theta = 90^{\circ}$

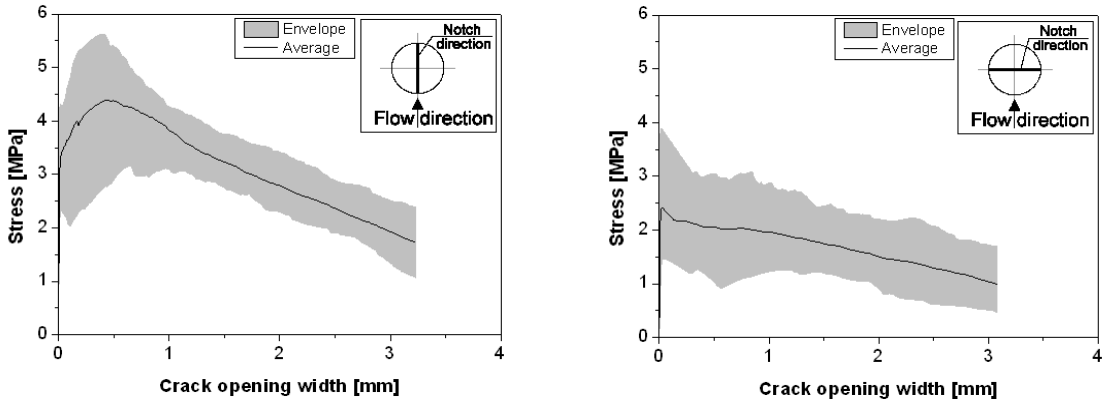

Figure 4: Nominal tensile stress – crack opening width relationship for SCC2: (a) $\theta = 0^{\circ}$ and (b) $\theta = 90^{\circ}$

Generally, the σ – w responses exhibited a relatively high scatter with the exception of the SCC1 series with θ = 90º (Figure 3b). In SFRC this type of scatter is generally high, even in specimens with the same casting and testing conditions, due to the high dependence of the post-cracking behaviour on the fibre distribution and orientation. Since the specimens were now extracted from distinct slab locations and at different distances from the casting point, an increase of scatter was expected. In fact, even when SCC requirements are assured based on the conventional test apparatus for measuring filling and passing abilities of a SCC, as well as resistance to segregation, the viscous nature of SFRSCC interferes with the distribution of the concrete constituents along the flow process, especially with steel fibres due to its higher aspect ratio.

By comparing Figures 3a and 3b, and Figures 4a and 4b, respectively, it is noticed that the influence of the notch orientation towards the concrete's flow on the post-peak behaviour of the material is quite high for the SCC2 series. These differences become more visible by comparing residual stresses and dissipated energies for each series. Tables 4 and 5 include the residual stresses and toughness parameters for different average crack opening mouth displacement for SCC1 and SCC2 series, respectively. In these tables σ_{max} is the maximum stress, $\sigma_{0.3}$, σ_1 and σ_3 are the residual stresses at a crack opening width of 0.3, 1 and 3 mm, respectively, and G_{F1} and G_{F3} are dissipated energy up to a crack opening width of, respectively, 1 and 3 mm. The G_{FX} is the area under the average σ – w curve up to X mm. Additionally, the coefficient of variation, CoV, and the characteristic values for a confidence interval of 95%, $k_{95\%}$, are included.

Table 4: Residual stress and toughness parameters obtained from indirect tensile tests for SCC1 (residual stress in MPa, and fracture energy in N/mm)

	$\theta = 0^{\circ}$ ($\sigma_{\parallel}$)*							$\theta = 90^{\circ}$ ($\sigma_{\perp}$)*					
	σ_{max}	$\sigma_{0.3}$	σ_1	σ_3	G_{F1}	G_{F3}		σ_{max}	$\sigma_{0.3}$	σ_1	σ_3	G_{F1}	G_{F3}
Average	4.23	4.08	2.32	0.71	3.17	6.26	**Average**	3.69	3.48	1.89	0.68	2.73	4.81
CoV(%)	19.9	21.3	20.1	46.6	19.1	20.6	**CoV(%)**	8.20	10.41	10.8	39.7	7.65	10.4
$K_{95\%}$	3.49	3.23	1.9	0.46	2.61	5.07	$K_{95\%}$	3.67	3.11	1.54	0.41	2.53	4.34

* ∥ and ⊥ - notch direction parallel (θ = 0º) and perpendicular (θ = 90º) to the concrete flow direction, respectively.

Table 5: Residual stress and toughness parameters obtained from indirect tensile test for SCC2 (residual stress in MPa, and fracture energy in N/mm)

	θ = 0º ($\sigma_{\parallel}$)							θ = 90º ($\sigma_{\perp}$)					
	σ_{max}	$\sigma_{0.3}$	σ_1	σ_3	G_{F1}	G_{F3}		σ_{max}	$\sigma_{0.3}$	σ_1	σ_3	G_{F1}	G_{F3}
Average	4.39	4.23	3.82	1.93	3.69	8.77	**Average**	2.42	2.13	1.96	1.04	2.21	5.30
CoV(%)	25.6	29.7	24.3	35.9	27.2	24.1	**CoV(%)**	33.1	48.6	37.9	34.9	35.9	31.0
$K_{95\%}$	3.52	3.16	2.09	1.34	3.05	7.42	$K_{95\%}$	2.07	1.74	1.46	0.74	1.59	4.03

As shown in Table 4, for the SCC1 series, the residual parameters are not significantly affected by the orientation of the notch. This can be due to the lower concrete viscosity in the fresh state that led to some segregation in this casting, resulting on a smaller effect on the fibre orientation. Moreover, in this batch, since casting from the centre point was unable to properly fill the mould, fibres tend to be oriented more randomly and less affected by the dynamic effect of the concrete's flow. From another point of view, it should not be ignored that the number of the specimens, which failed during test after the crack initiation was higher due to the inappropriate distribution of the fibres within the slab. Most of these specimens were located near the corners of the slab, and it could be concluded that due to the segregation of the aggregates and fibres more paste had moved to the corner locations.

In Table 5, the θ = 0º series shows higher residual stresses for higher crack widths and also higher dissipated energy comparing to the specimens of θ = 90º of SCC2 series. This variation in the residual parameters could be ascribed to a preferential orientation of the fibres at the fracture surface. As it will be discussed in more detail further ahead, during the casting stage, fibres could tend to be aligned perpendicular to the direction of concrete flow, maybe due to a uniform radial velocity profile. Therefore, for the specimens with the notched plane parallel to the flow direction, more fibres are perpendicular to the crack plane, and consequently, a higher number of fibres intersect more effectively the fracture surface.

When comparing the post-cracking stresses and toughness for higher crack widths, i.e.1 mm, of the SCC1 and SSC2 series, a significant increase was observed for SCC2, which had lower compressive strength. Reduction in the matrix compressive strength raises residual stresses and consequently dissipated energy. This increment is also visible by comparing Figures 3 and 4. In Figure 3 after reaching the maximum stress, a sudden reduction in the stress is observed while this reduction in Figure 4 is much smoother. For instance, the average residual stresses, at a 1 mm crack width are $\sigma_{\parallel}$=2.32 MPa and $\sigma_{\perp}$=1.89 MPa for SCC1, and $\sigma_{\parallel}$=3.82 MPa and $\sigma_{\perp}$=1.96 MPa for SCC2.

3 ASSESMENT OF FIBRE DISTRIBUTION AND ORIENTATION

To determine the mechanical properties of fibre reinforced composite materials, it is quite important to identify the fibre orientation. Depending on the fibre orientation in a certain composite, usually given by a fibre orientation factor, η, the number of fibres bridging a crack may be somehow distinct. However, this factor changes for distinct situations and may also be influenced by the concrete flow [14]. For a FRC, since the overall composite behaviour is strongly affected by the fibre density and orientation, consequently, it is feasible to expect an anisometric material behaviour for this kind of composites. For example, experimental results reveal that the fibres tend to segregate in the plane perpendicular to the gravity field during compaction [15,16], hence the material residual strength will vary with the element's depth. Previous research showed that the concrete toughness is influenced by the number of effective fibres in the crack section. Nevertheless, the number of the effective fibres, also designated as fibre effectiveness index by many researchers, depends on the fibre dosage, fibre orientation and the length efficiency factor [17]. Soroushian and Lee [18] computed the average orientation factor from Equation (2),

$$\eta = N^f . \frac{A_f}{V_f} \qquad (2)$$

where, V_f and A_f represents the volumetric fraction of fibre (in %) and the cross sectional area of a single fibre (in mm^2), and N^f is the number of fibres intersecting a certain plain.

Table 6 includes the fibre density determined, after testing, by counting fibres at the facture surface, where $N_{\shortparallel}^f$ and $N_{\perp}^f$ are, respectively, the fibre density at a crack plane parallel and perpendicular to the concrete flow. Additionally, it is also included the orientation factor at the fracture surfaces parallel and perpendicular to the concrete flow, respectively, $\eta_{\shortparallel}$ and $\eta_{\perp}$. These factors were computed by introducing the experimental fibre densities $N_{\shortparallel}^f$ and $N_{\perp}^f$ into Equation 2. In each row are included specimens with the same distance from the casting origin. Regarding each studied distance, the number of the fibres was assessed in two perpendicular planes (parallel and perpendicular to the concrete flow direction). For SCC2 series, the fibre density was considerably higher at the specimens with θ=0º, approximately 49% when comparing to specimens with θ=90º. This high variation of the fibre density in two perpendicular directions for SCC2, can be due to the preferential orientation and also dispersion of the fibres during the concrete flow. For the SCC1 series, the variation of the fibre density in the two orthogonal sections was negligible. This could be due to the lower concrete viscosity and the improper filling of the mould, which led to a more randomly fibre distribution. The expected theoretical fibre densities for either a 2D or 3D situation, $N^{f,2D}$or $N^{f,3D}$, can be computed from Equation 2, by adopting either a 2D or 3D isotropic uniform random distribution, respectively, $\eta^{2D} = 2/\pi$ and $\eta^{3D} = 0.5$. For SCC1, the expected theoretical fibre densities are $N^{f,2D} = 2.22$, $N^{f,3D} = 1.74$, while for SCC2 they are $N^{f,2D} = 2.06$ and $N^{f,3D} = 1.62$. The average density assessed experimentally was lower than the expected theoretical density for a 2D isotropic uniform random distribution. Since the specimen's fibre density was assessed after testing, at the fracture surface, it could have been an improper counting of fibres, due to fibre rupture. A more conclusive idea of the actual fibre density and orientation factor could be withdraw from an image analysis of cut planes from the SFRSCC panel.
It was observed a decrease on the average value of η from the parallel to the perpendicular sections in the case of SCC2. No significant variation was observed for SCC1. These observations show that for the more workable concrete (SCC2), the fibres will be preferentially aligned perpendicular to the concrete flow direction.

Table 6: Fibre density on the fracture surface of each specimen (the number of fibres is shown in fibres/cm^2)

		SCC1				**SCC2**			
Distance (cm)	**Specimen**	$\mathbf{N_{\shortparallel}^f}$	$\mathbf{N_{\perp}^f}$	$\boldsymbol{\eta_{\shortparallel}}$	$\boldsymbol{\eta_{\perp}}$	$\mathbf{N_{\shortparallel}^f}$	$\mathbf{N_{\perp}^f}$	$\boldsymbol{\eta_{\shortparallel}}$	$\boldsymbol{\eta_{\perp}}$
0	O	1.46	NA	0.37	NA	1.15	NA	0.29	0.20
20	B2, B3	NA	NA	NA	NA	1.18	0.36	0.30	0.09
23.5	A3, A4	1.03	1.35	0.26	0.34	0.99	0.48	0.25	0.12
32	C3, C4	NA	0.92	NA	0.23	1.12	0.54	0.28	0.14
32	D3, D4	0.67	0.80	0.17	0.20	1.22	0.60	0.31	0.15
40	B1, B4	0.86	0.74	0.22	0.19	1.41	0.31	0.36	0.08
46.5	A2, A5	1.15	1.35	0.29	0.34	0.82	0.50	0.21	0.13
56	C2, C5	1.18	NA	0.30	NA	1.19	0.46	0.30	0.12
56	D2, D5	1.17	0.95	0.30	0.24	1.06	0.43	0.27	0.11
69.5	A1, A6	0.98	1.05	0.25	0.27	1.30	0.30	0.33	0.08
77.5	C1, C6	1.10	0.88	0.28	0.22	0.77	0.69	0.19	0.17
77.5	D1, D6	0.71	1.27	0.18	0.32	1.10	0.80	0.28	0.20
Minimum		0.67	0.74	0.17	0.19	0.77	0.30	0.19	0.08
Average		1.03	1.03	0.26	0.26	1.11	0.52	0.28	0.13
CoV (%)		23.08	22.68	23.08	22.69	16.48	32.63	16.49	32.63

NA - specimen fail either during extracting from panel or during testing.

Figure 5 depicts the relationship between the residual tensile strength, σ_R, and the number of the fibres counted at the notch fracture surface of the specimens after performing the indirect tensile test. It is observed, as expected, that residual strength have a tendency to increase with the number of fibres bridging the fracture surface, being this effect more pronounced in the σ_{max} and σ_1. The residual stress for a 3 mm crack width (σ_{3mm}) increased at a considerably lower rate in the SCC1 series. This is mainly due to the fibre rupture that has occurred more often in the SCC1 series.

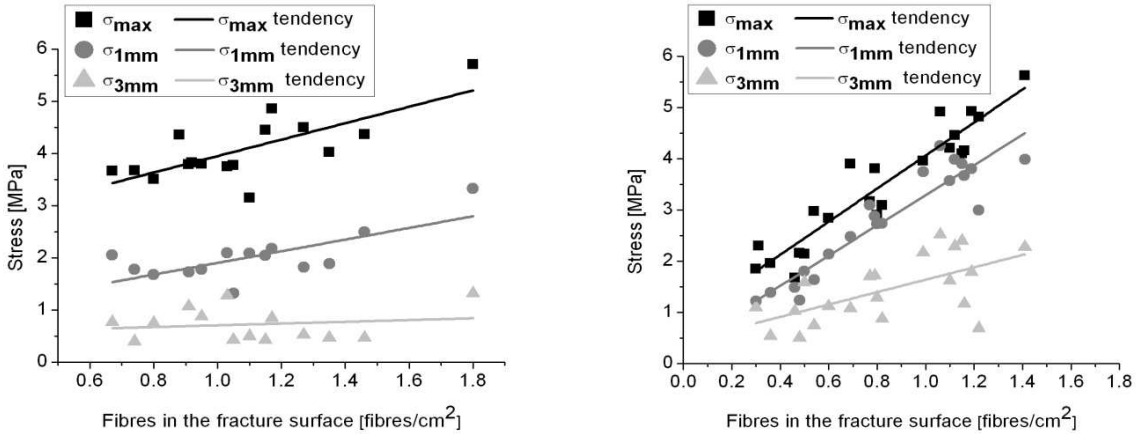

Figure 5: Relationship between the residual tensile stress and the number of fibres found in the notched fracture surfaces of specimens: (a) SCC1 (b) SCC2

In Figure 6, the relationship between the residual tensile stress and distance from the casting point (centre of each panel) are depicted. For the both series, residual stresses are divided into two categories, where σ_{II} represent residual stress in the specimens with $\theta=0^o$ and $\sigma_{\perp}$ shows residual stress in the specimens with $\theta = 90^o$. It is observed that, in both series, with increasing distance from the casting point residual stresses are not affected importantly.

Figure 7 depicts the relationship between the number of the fibres at the notched fracture surfaces and distance from the casting point. As it is expected, for SCC1, due to segregation, the number of fibres has decreased with the increase of the distance from the casting point. On the other hand, for the SCC2 series a good homogeneity and distribution of the fibres through the panel was achieved.

Several researchers suggested that the fibres within a self-compacting matrix tend to align in the direction of the concrete flow [3,4,19]. During the casting process, fibres are reoriented due to the variation in the flow velocity profile. Stahli et al. [18] suggested a simplified justification for the reason of the fibres alignment, see Figure 7. In this flow profile, the velocity of concrete flow is high in the centre of the channel and reduces with becoming closer to the walls of formwork due to the frictional resistance between concrete and wall. Variation in the concrete flow velocity forces fibres to reorient parallel or perpendicular to the concrete flow direction (depends on the mould's shape and also casting location).

In the authors' opinion, in the case of casting slabs the flow velocity profile is completely different. Since in the casting process of the panels, particularly from the centre, the wall effects are negligible, hence the flow velocity is uniform and diffuses outwards radially from the casting point, see Figure 9. This effect is stronger at the higher flow velocity or, on the other hand, a more workable concrete such as SCC2. The same profile had been observed by [20,21].

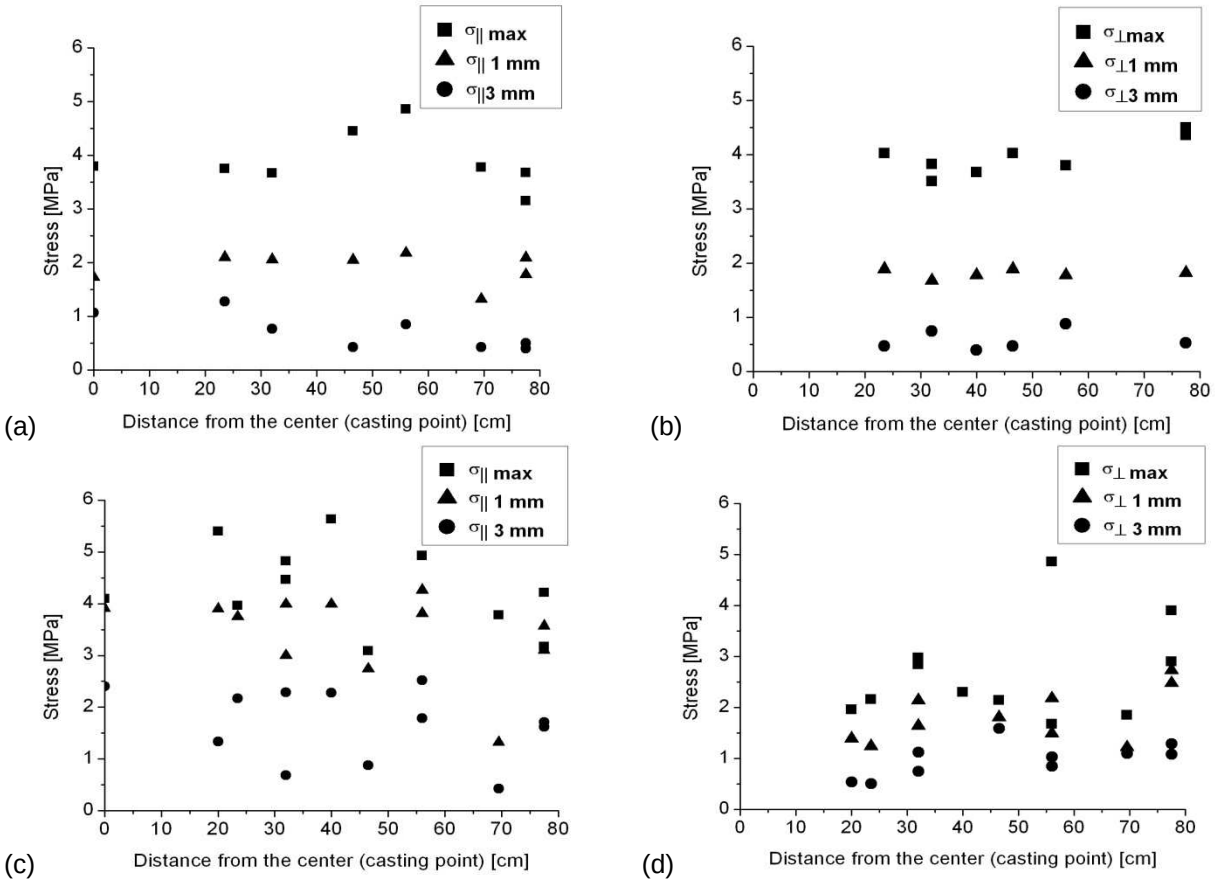

Figure 6: Relationship between the residual tensile stress and distance from the centre of each panel: (a) For SCC1 and θ=0º; (b) For SCC1 and θ=90º; (c) For SCC2 and θ=0º and (d) for SCC2 and θ=90º

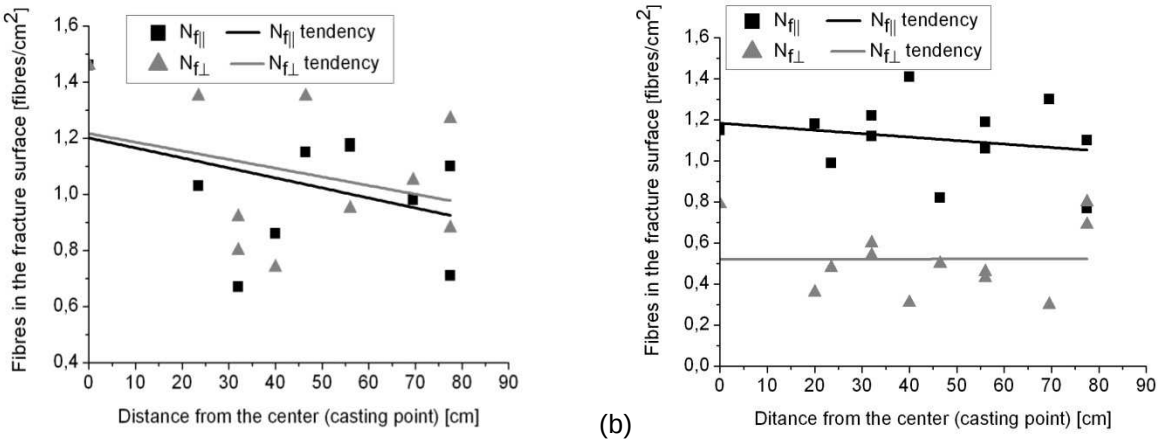

Figure 7: Relationship between the number of fibres found in the notched fracture surfaces and distance from the centre of each panel: (a) SCC1, (b) SCC2

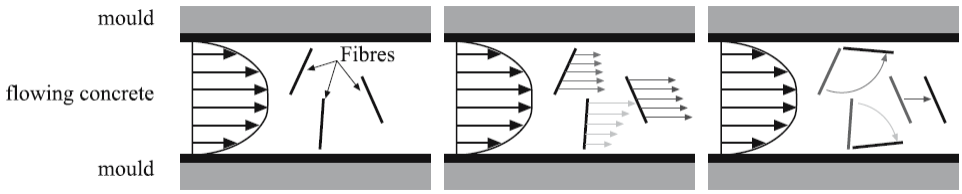

Figure 8: Explanation for fibre alignment in flowing concrete of channel [19]

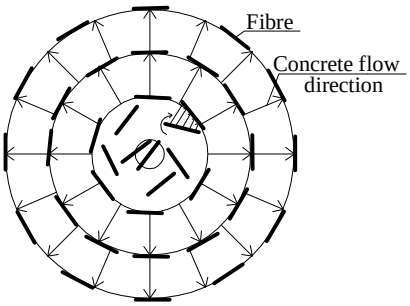

Figure 9: Explanation for fibre alignment in flowing concrete of a slab casting from the centre

4 CONCLUSION

In this work, the influence of fibre dispersion and orientation on the post-cracking behaviour of the steel fibre reinforced self-compacting concrete was assessed by indirect (splitting) tensile test. The specimens were extracted from distinct locations in panel prototypes. Two self-compacting mixtures were prepared using the same base mix proportions.

Fresh state properties of concrete were found to strongly affect dispersion and orientation of fibres and, consequently, mechanical performance of SCC. It was found that fibres tend to orient perpendicular to the concrete flow direction. The series with lower compressive strength has shown better post-cracking behavior than the one with the higher compressive strength. In the proposed mix designs, it seems that SCC2 was more efficient since pullout fibre reinforcement mechanisms were fully mobilized during the crack propagation process. For series with higher compressive strength (SCC1), due to the stiffer bond between matrix and fibre interface, fibres ruptured more often, consequently lower residual strengths and toughness were achieved.

The fibre density/orientation was found to have a very significant effect on the tensile behaviour of the concrete slabs. In the case of the casting panels from the centre, the flow profile velocity may be uniform and diffuses outwards radially from the casting point, and a tendency to have higher number of fibres orthogonal to the concrete flow direction was observed in the mix with better SCC requisites.

5 AKNOWLEDEGMENT

The studies reported in this paper are part of the research program LEGOUSE (Qren, project nº 5387). The materials were supplied by Radmix and Maccaferri (fibres), SECIL (cement), SIKA and BASF (superplasticizers), Omya Comital (limestone filler), and Pegop (Fly ash).

REFERENCES

[1] K.M.A. Hossain, M. ASCE, M. Lachemi, **"**Bond behavior of self-consolidating concrete with mineral and chemical admixtures**"**, Int. J. Mater. Civi. Engng*, ASCE*, 20, 9, 608-616 (2008).

[2] J.F. Lataste, M. Behloul, D. Breysse, **"**Characterization of fibres distribution in a steel fibre reinforced concrete with electrical resistivity measurements**''**, NDT&E Int., 41, 638-647 (2008).

[3] L. Ferrara, N. Ozyurt, M.D. Prisco, **"**High mechanical performance of fibre reinforced cementitious composites: the role of "casting-flow induced" fibre orientation'', J. Mater. Struct., 44, 109-128 (2011).

[4] M.C. Torrijos, B.E. Barragan, R.L. Zerbino, **"**Placing conditions, mesostructural characteristics and post-cracking response of fibre reinforced self-compacting concretes**''**, Const. Build. Mater., 24, 1078-1085 (2010).

[5] A.G. Kooiman, *Modeling steel fibre reinforced concrete for structural design*, PhD Thesis, department of structural and building engineering, Delft University of technology, 2000.

[6] B. Big, M.K. Lee, **"**Round-robin analysis of the RILEM TC 162-TDF beam – bending test: Part 3 – fibre distribution'', Mater. Struct. ,36 ,631-635 (2003).

[7] F.L. Oliveira, *Design-oriented constitutive model for steel fiber reinforced concrete*. PhD thesis. Universitat Politècnica de Catalunya, 2010.

[8] L. Martinie, P. Rossi, N. Roussel, **"**Rheology of fiber reinforced cementitious materials: classification and prediction'', 08, 032, (2009).

[9] D. Dupont, L. Vandewalle, **"**Distribution of steel fibres in rectangular sections'', Cem. Con. Com., 27, 391-398 (2005).

[10] S.P. Timoshenko and J.N. Goodier, *Theory of Elasticity*. McGraw-Hill, New York, 1991.

[11] C. Rocco, G.V. Guinea, J. Planas, M. Elices, **"**Review of the splitting-test standards from a fracture mechanics point of view''. Cem. Con. Res., 31, 73-82 (2000).

[12] EFNARC, "The European guidelines for self-compacting concrete". May 2005.

[13] ASTM C 496, "Standard test method for splitting tensile strength of cylindrical concrete specimens". December, 2006.

[14] V.M.C.F. *Cunha Steel Fiber Reinforced Self-Compacting Concrete (from Micro-Mechanics to Composite Behaviour)*, PhD Thesis, University of Minho, 2010.

[15] P. Stroeven, **"**The analysis of fibre distribution in fibre reinforced materials'', J. Microsc: Part 3, 111, 283 (1977).

[16] P. Stroeven, **"**Morphometry of fibre reinforced cementitious materials, Part II: Inhomogeneity, segregation and anisometry of partially oriented fibre structures'', Mater. Const., 12, ,9-20 (1979).

[17] P. Stroeven, **"**Effectiveness of steel wire reinforcement in a boundary layer of concrete'', Acta. Stereol., 10, 113-122 (1991).

[18] P. Soroushian and C.D. Lee, **"**Distribution and orientation of fibers in steel fiber reinforced concrete'', ACI Mater. J., 87, 433-439 (1990).

[19] P. Stahli, R. Custer, J.G.M. Mier, **"**On the flow properties, fibre distribution, fibre orientation and flexural behaviour of FRC'', J. Mater. Struct., 41, 189-196 (2008).

[20] B. Boulekbache, M. Hamrat, M. Chemrouk, S. Amziane, **"**Flowability of fibre-reinforced concrete and its effect on the mechanical properties of the material'' Const. and Build. Mater., 24, 1664-1671 (2010).

[21] S.J. Barnett, J.F. Lataste, T. Parry, S.G. Millard, M.N. Soutsos, **"**Assessment of fiber orientation in ultra-high performance fibre reinforced concrete and its effects on flexural strength'' *J. Mater. Struct.*, 43, 1009-1023 (2010).